Zeitschrift für Geomorphologie, Supplementary Issue **Fast Track Article**
Published online January 2013

Roughness determination of coarse grained alpine river bed surfaces using Terrestrial Laser Scanning data

Henning Baewert, Martin Bimböse, Alexander Bryk, Eric Rascher, Karl-Heinz Schmidt and David Morche

with 8 figures and 2 tables

Abstract. Channel bed roughness principally controls flow resistance in gravel bed rivers. Direct measurement of streambed surface roughness however remains a difficult problem in fluvial geomorphology. The conventional methods for measuring bed roughness often require an exact knowledge of grain size distributions throughout a given stream reach and thus rigorous grain size analysis. This may be impractical for large catchments, and systems containing a large degree of form roughness. Surface characterization using terrestrial laser scanning (TLS) addresses these problems. The ultimate goal of this research is to improve upon the methods for roughness length determination in gravel-bed rivers using TLS. To this end, two principle methodological considerations were examined. 1.) The influence of the number of scan positions on roughness calculation. 2.) The influence of grid-cell size on roughness calculation during post-processing. Scan data were furthermore compared to sediment samples to relate TLS-data to conventional roughness calculation methods. Several test sites in the Reintal valley, Bavaria, Germany were scanned from multiple orientations. The results from these experiments show that despite minor particle shading, roughness length determination does not depend significantly on the number of scan orientations used. However, results clearly show that roughness length determination depends highly on the choice of grid cell size during post processing. This study supports the use of TLS as the most appropriate and versatile method for roughness analysis in gravel bed rivers.

Key words: channel bed roughness, terrestrial laser scanning, grain size, alpine river, Reintal

1 *Introduction*

Frictional resistance is a highly variable factor in natural channels as it depends on both the flow conditions (e.g., discharge, Reynolds Number, Froude Number) as well as channel boundary conditions (e.g., bed roughness and cross-sectional geometry). Streambed roughness exerts a dominant control on flow resistance and thus widely influences water stage, local velocity and sediment transport. Many previous studies have focused on the relationship between streambed roughness and flow resistance. Nikuradse's seminal work in pipe flow (Nikuradse 1933) experimentally showed the direct influence of roughness on flow conditions. Gomez (1993) and Smart et al. (2004) dealt with the measurement of surface roughness in coarse grained channels. Hey (1979), Lee & Ferguson (2002), Aberle & Smart (2003), Comiti et al. (2009) and Robert (2011) concentrated on bed-surface structure and its influence on flow resistance. Despite the amount of attention directed toward flow resistance in natural channels and the importance of this for flood risk management and hydrogeomorphological modeling there is still a lack of detailed understanding on the interactions between bed roughness and river flow.

www.borntraeger-cramer.de
DOI: 10.1127/0372-8854/2013/00127 0372-8854/13/00127 $ 0.00

In mountain streams flow resistance is primarily generated by channel bed roughness (Hey 1979, Montgomery & Buffington 1997). In general, bed roughness is divided into grain roughness and form roughness (Reid & Hickin 2008). Grain roughness is determined by the surface grain size distribution and by the protrusion of particles into the flow (Heritage & Milan 2009, Robert 2011). Form roughness may be caused by several features such as transverse ribs, gravel bars and step-pool-sequences (van Rijn 1984, Smart et al. 2004) or large organic debris (Eitelmann & Morche 2011).

Usually, bed roughness calculation utilizes a specific percentile (e.g., D_{50}, D_{84}) of the grain-size distribution (Boyer 1954, Bathurst 1985, Gomez 1993, Lee & Ferguson 2002). This approach inevitably contains complications (see Heritage & Milan 2009). For example, particle protrusion and grain packing are not considered. In addition, experimental studies (e.g., Bathurst 1985, Gomez 1993) have shown bed roughness to be dominantly determined by the shortest principle axis. This suggests, roughness determination via the grain size and thus via the intermediate axis may be inappropriate. More promising methods in determining the roughness are the random field approach in combination with terrestrial laser scanning. The random field approach (Furbish 1987, Nikora et al. 1998) is a method that can be used to calculate bed roughness. When utilizing this method, the study site is considered as a field of randomly distributed heights (z) each associated with a position (x, y). This approach has advantages, such as quantifying the in situ roughness height including partial burial, grain packing and particle imbrication. The application of TLS to create high resolution topographic data has been increasingly used recently for channel morphology research (Heritage & Hetherington 2005, 2007, Milan et al. 2007, Heritage & Milan 2009, Hodge et al. 2009, Pignatelli et al. 2010) and has enhanced quantification techniques like the random field approach. However, the use of laser scanning data to quantify bed surface roughness has led to new methodological problems. Parts of the channel surface situated behind a large obstacle cannot be surveyed. This is known as the "shading effect". This problem requires the study site to be scanned from different angles in order to produce a complete 3-D image of the surface. The first goal of this study is to determine the minimum number of scan positions required to accurately characterize the channel bed roughness.

For surface roughness calculation, the study site is divided into an orthogonal grid with cell sizes defined by the largest particle in the test area (Heritage & Milan 2009). This requires sediment sampling and leads to additional labor intensive field work. In an effort to avoid this, this study further assesses the importance of grid cell size on bed roughness calculation. For this reason, sediment samples were collected from scanned areas. Finally, these samples were also used to compare TLS-derived surface topography to conventional methods for roughness calculation.

The ultimate goal of this research is to enhance the application of TLS data for the calculation of bed surface roughness of a coarse grained alpine river. Two study sites in the Reintal valley, Bavaria, Germany were chosen for analysis – one for each examined methodological consideration outlined above.

2 *Study area*

The investigation area is situated in the Reintal valley located in the northern limestone Alps (Wettersteingebirge) Bavaria, Germany (Fig. 1). Recently, the Reintal valley was intensely inves-

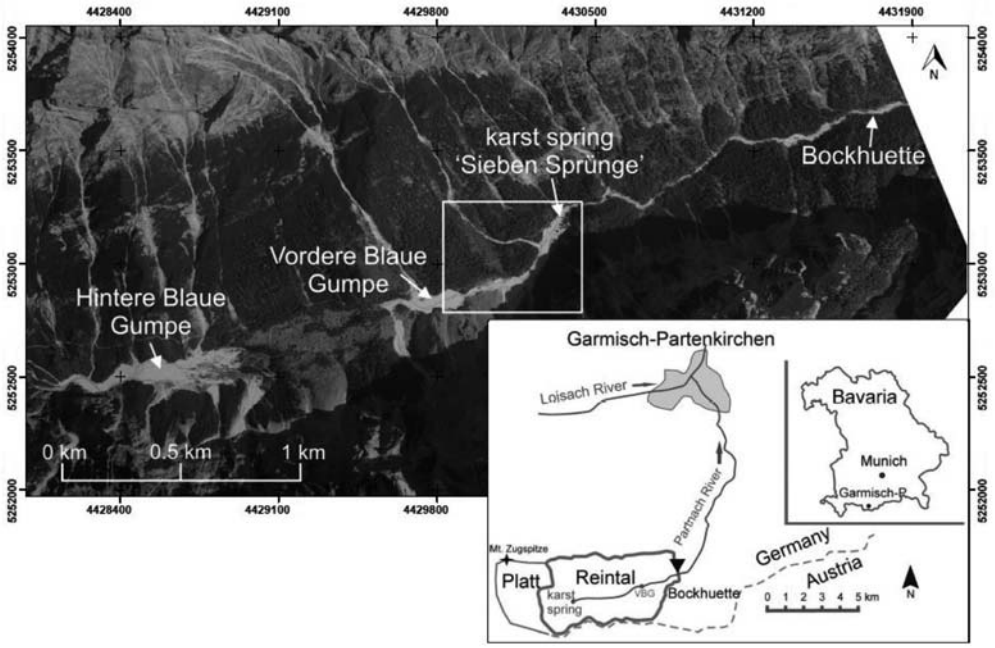

Fig. 1. Location of the study area Reintal valley (the black triangle marks the gauging station Bockhuette, VBG = Vordere Blaue Gumpe, the white box marks the area were the two study sites are located); coordinate system: Germany (zone 4), transverse mercator projection. (background: © Landesamt für Vermessung und Geoinformation Bayern permission to use and publication from 28 July 2004, reference number: VM3831B-oN/2600).

tigated in several geomorphological research projects with a focus on the function and coupling of sediment sources and stores as well as the sediment transfer in an alpine sediment cascade (among others Schmidt & Morche 2006, Schrott et al. 2006, Heckmann et al. 2008, Bimböse et al. 2011, Heckmann et al. 2012, Krautblatter et al. 2012). A detailed geomorphological description of the Reintal valley can be found in Götz & Schrott (2010). The valley is drained by the Partnach River, a tributary of the Loisach River. At the gauging station Bockhuette the Partnach River drains 27 km^2. Two large historic landslides dammed the Partnach River creating two small lakes (Vordere Blaue Gumpe and Hintere Blaue Gumpe) and divided the valley into several subcatchments (Morche et al. 2006, Sass et al. 2007). After each ablation period the lakes run dry and the Partnach River flowed subterranean and came to the surface again at the karst spring "Sieben Sprünge" (Fig. 1). The lakes were subsequently filled with sediments and large alluvial plains developed. The grain size characteristics of the Vordere Blaue Gumpe (VBG) plain were investigated by Morche & Schmidt (2005). They determined a D_{84} of 40 mm (coarse gravel) for the surface particles. During a 6-year (2000–2005) geodetic survey Morche et al. (2006) measured the annual lake infill by bed load of the Partnach River. Between 2000 and 2004 the mean annual bed load transport in the Gumpe subcatchment was about 950 t. This value is more than one magnitude higher than the bed load export out of the Reintal valley at gauging station Bockhuette

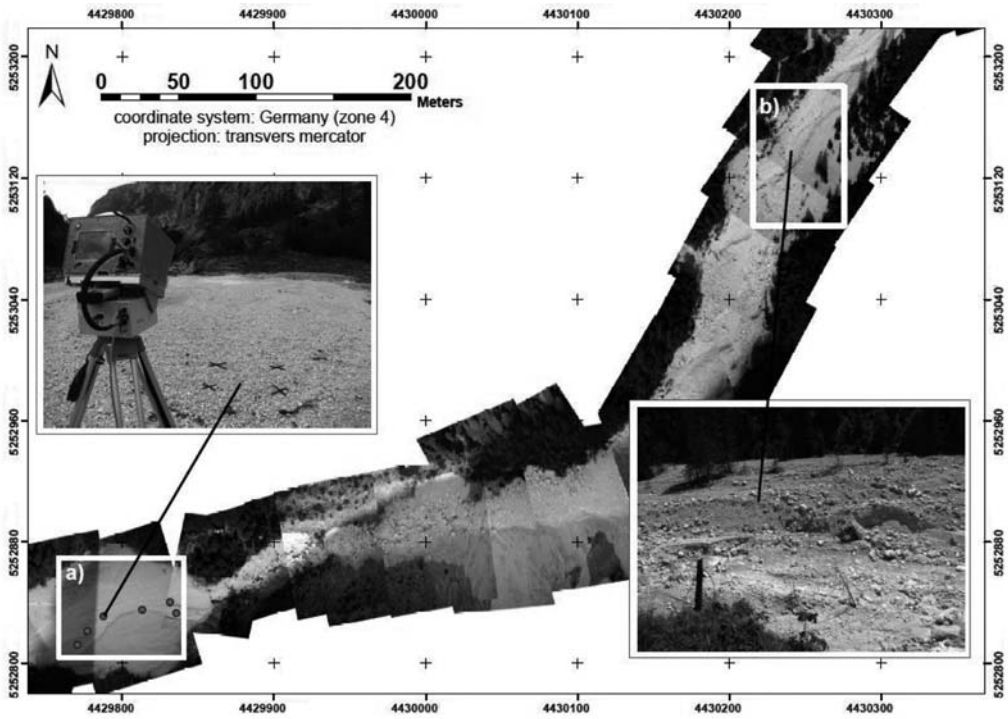

Fig. 2. Location of the two study sites in the Reintal valley. The white boxes mark the different study sites. inset a) study site Gumpe with 6 test sites; the upper left photograph shows test site 3; inset b) study site Sieben Sprünge, lower right photograph: riffle-pool sequence and fluvial terraces at study site Sieben Sprünge.

in the same observation period (Schmidt & Morche 2006, Morche et al. 2008) showing the high geomorphic connectivity of the slope system to the fluvial system in terms of coarse sediment flux in the Gumpe area.

The Vordere Blaue Gumpe landslide dam failed between 22–23.08.2005 during heavy rain. The sudden lake outflow caused a flood wave. As a result, a large amount of sediment (approx. 100,000 t) was mobilized in the downstream channel reach of the Partnach River (Morche et al. 2007). Since the dam failed, the VBG alluvial plain has been intimately coupled to the Partnach River in terms of sediment input and temporary storage (Morche et al. 2006, Morche & Schmidt 2012). In the first years after the dambreak flood the river load dominance was shifted from dissolved load to bed load (Morche & Schmidt 2012). Bimböse et al. (2011) have surveyed the alluvial plain of the Gumpe by terrestrial laser scanning in 2008 and 2009. They could quantify the net sediment export out of the Gumpe area, 438 m^3 in 2008 and 229 m^3 between 2008 and 2009.

Two study sites were chosen within the Reintal valley (Fig. 2). The first study site (Fig. 2, inset a) was selected to assess the influence of the number of scans on roughness calculation. It is located on the alluvial plain of the VBG and six test sites were investigated in greater detail (see below).

The second study site (study site Sieben Sprünge, Fig. 2, inset b) is located in a channel reach 600 m downstream of the study site Gumpe. This area was heavily affected by the August 2005

flood as large fluvial terraces (up to several meters) were deposited there (see also Fig. 8 in MORCHE et al. 2007). This site was chosen to address the issue concerning grid cell size for roughness length calculation.

3 *Methods*

Particle samples (n = 100) from each test site were taken randomly to compare with scanner-derived data. Two methods of sampling were used. The sampling frame method (BUNTE & ABT 2001) was used for the six test sites at the VBG (study site Gumpe, Fig. 2, inset a). The sampling frame was divided into nine equal grid cells. From each cell, 11 particles were sampled with the final particle chosen from a random grid cell. For study site Sieben Sprünge (Fig. 2, inset b), the classic line-by-number method was used (WOLMAN 1954). The three axes (longest = a-, intermediate = b-, shortest = c-axis) of each particle were determined using a ruler. Particle samples were then used to determine the grain-size distribution including the characteristic grain sizes D_{50} and D_{84}. Additionally, Cumulative Distribution Functions (CDF) from the shortest axis (c-axis) were created grouping values in 5 percent intervals. These data were used to compare conventional sampling methods with the scanner-derived data (HERITAGE & MILAN 2009).

At study site Gumpe, six 1 × 1 m test sites were selected to analyse surface roughness using terrestrial laser scanner data. To avoid particle shading each test site was scanned from five different positions. The mean distance between test site and laser scanner was 5.45 m. This distance was chosen for two reasons: first, a minimum distance of three meters must be maintained between laser scanner and scanned object (OPTECH 2012). Second, the beam divergence and point spacing increase with distance causing resolution problems. For example, the point spacing of the ILRIS-3_6D is about 1.8 mm at a distance of 100 m and the corresponding beam diameter is about 29 mm. This leads to a partial overlap of the laser beam, resulting in an error in the returning signal (PESCI et al. 2011). For the ILRIS-3_6D scanner used in this study, beam divergence is calculated after PESCI et al. (2011). The point spacing for all scans of the test sites were between 1.9–2.7 mm and the corresponding footprint at the target was between 12.78–13.06 mm.

For study site Sieben Sprünge a larger river reach was scanned. Contrary to study site Gumpe, this site was recorded from only one position due to its inaccessibility from other locations. To minimize the shading effect the laser scanner was positioned at approximately 5 m above bed surface. Study site Sieben Sprünge was scanned with a point spacing of 12.52 mm at a distance of approximately 31 m. The footprint at the target was 17.32 mm. For all scans the last pulse mode was chosen to eliminate extraneous data points ensuring that only points from the ground surface were recorded.

After obtaining raw data, all scans were converted to the PolyWorks file format for data processing. Raw scan data were then internally referenced using a minimum of three manually selected common points. An Iterative Closest Point (ICP) algorithm implemented in PolyWorks (Best-fit Alignment & Comparison) was then applied to merge the point clouds automatically. For a detailed discussion on the merging procedure see BUCKLEY et al. (2009), CONFORTI et al. (2005), PESCI et al. (2007) and RABATEL et al. (2008). For each test site, multiple point cloud merging combinations (10 in total) were constructed from the original five scans. Each individual scan was used to generate a corresponding data set (1scan_a, 1scan_b, 1scan_c, 1scan_d and 1scan_e). Additionally,

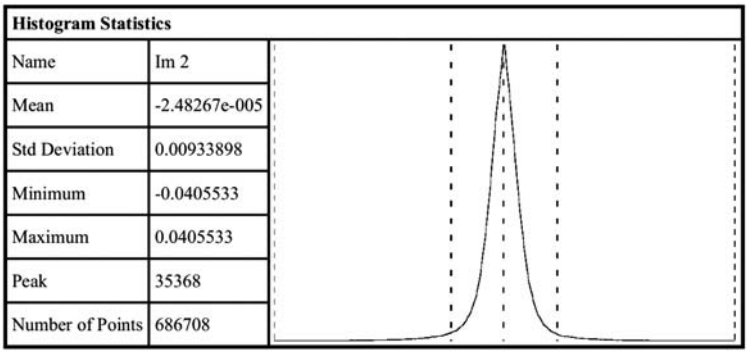

Histogram Statistics	
Name	Im 2
Mean	-2.48267e-005
Std Deviation	0.00933898
Minimum	-0.0405533
Maximum	0.0405533
Peak	35368
Number of Points	686708

Fig. 3. Histogram pane and statistics of the merging procedure of two scans from Gumpe test site 3.

two data sets were created by merging spatially opposed scans (2scans_a, 2scans_b). Finally, data sets consisting of three (3scans), four (4scans) and five (5scans) merged scans were generated. The standard deviation of the merging error was very different for the several test sites. For Gumpe test site 2, the standard deviation of the merging error was 5.5 mm to 6.1 mm. At Gumpe test site 1 the value was between 10 mm and 11.4 mm. The range of the standard deviation for Gumpe test site 6 is between 12 mm and 14.6 mm. The standard deviation for the remaining test sites is between 7.8 mm and 9.6 mm. A histogram pane of the merging error of Gumpe test site 3 is shown in Fig. 3.

These data were imported into the PolyWorks Software IMInspect for further analysis. To reduce the impact of slope on roughness calculation, the point clouds were projected onto a simple plane. The data were further cropped to fit a 1 m² areas for consistency. Finally, all data sets were exported to ASCII files for further interpretation.

The data-processing procedure for study site Sieben Sprünge was nearly the same. Due to the large size of the study site (about 90 m in width), multiple scan windows were merged together using PolyWorks (Best-fit Alignment & Comparison). The standard deviation of the merging error ranged between 19.2 mm and 20.8 mm.

To reduce slope effects on surface roughness calculation, a grid for every study site was created (Heritage & Milan 2009). For the first study site, the grid size was defined by the largest particle collected. For study site Sieben Sprünge the data were regridded at 0.1 m, 0.5 m and 1 m cell sizes producing three data sets. Subsequently, the point cloud data were assigned to the grid cell in which they were located.

The mean height and standard deviation were calculated for every grid cell. The first standard deviation is equivalent to the effective roughness height (h_r) (Heritage & Milan 2009). Subsequently, the mean and median values of the effective roughness heights were calculated for all data sets. The standard deviation between these mean values was used to show differences between the data sets (Table 1). From flume experiments, Gomez (1993) found that typically the longest axis (a-axis) of particles is orientated orthogonal to the flow direction, the intermediate axis (b-axis) is parallel to the flow and the shortest axis (c-axis) is perpendicular to the channel bed. Therefore, the c-axis may be the most important for surface roughness determination. Heritage & Milan (2009) further supposed that the c-axis was roughly twice the standard deviation of mean height

values. For this reason, the h_r values were multiplied by a factor of two and compared with c-axis values from collected samples (Table 2). Several large boulders located at study site Sieben Sprünge could not be measured during field work due to size and partial burial. In contrast, these boulders were included in the TLS derived data. Thus, in order to appropriately compare study site Sieben Sprünge and eliminate biasing due to large particles, 2 h_r outliers exceeding the 99th percentile were not considered in the regression analysis (see below).

4 *Results*

4.1 *Sediment samples*

The grain size distributions of the two study sites are displayed in Fig. 4. Study site Gumpe consisted of [illegible]% gravels ranging from 8 mm to 64 mm which is well in accordance with a previous study by MORCHE & SCHMIDT (2005). At all study sites the percentage of fine gravel was very small. The characteristic grain sizes D_{50} and D_{84} of Gumpe test sites 1 and 6 were larger than at the other test sites (Fig. 4). The finest particles were located at Gumpe test site 2. The sediments at study site Sieben Sprünge were similar to study site Gumpe, although the D_{84} at this site was twice as high (Fig. 4).

4.2 *TLS-derived data*

For all study sites the calculated mean values of h_r were larger than the median values. As a result, the roughness values exhibit a right-skewed distribution. For this reason, the median h_r value was used to quantify the average surface roughness. Fig. 5 shows all roughness grids for the "5scans" data set at study site Gumpe. Differences in grid cell size result from varying grain size distributions.

All data sets created within a given test site at study site Gumpe show similar results (Table 1). The median h_r values from different data sets at test site 1 are not significantly different as all scans

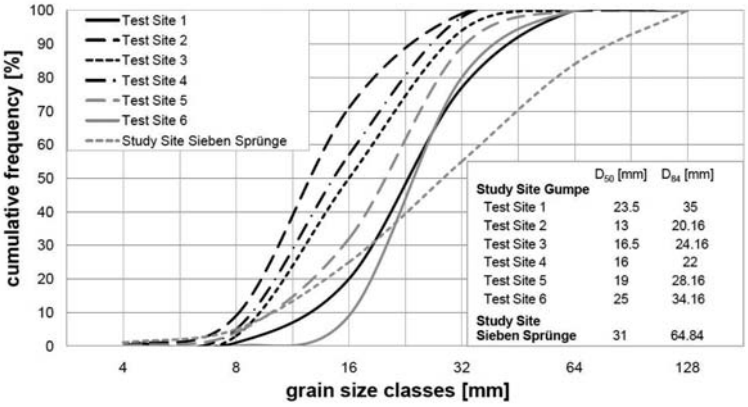

Fig. 4. Cumulative grain size distributions and characteristic grain sizes (D_{50}, D_{84}) for both study sites.

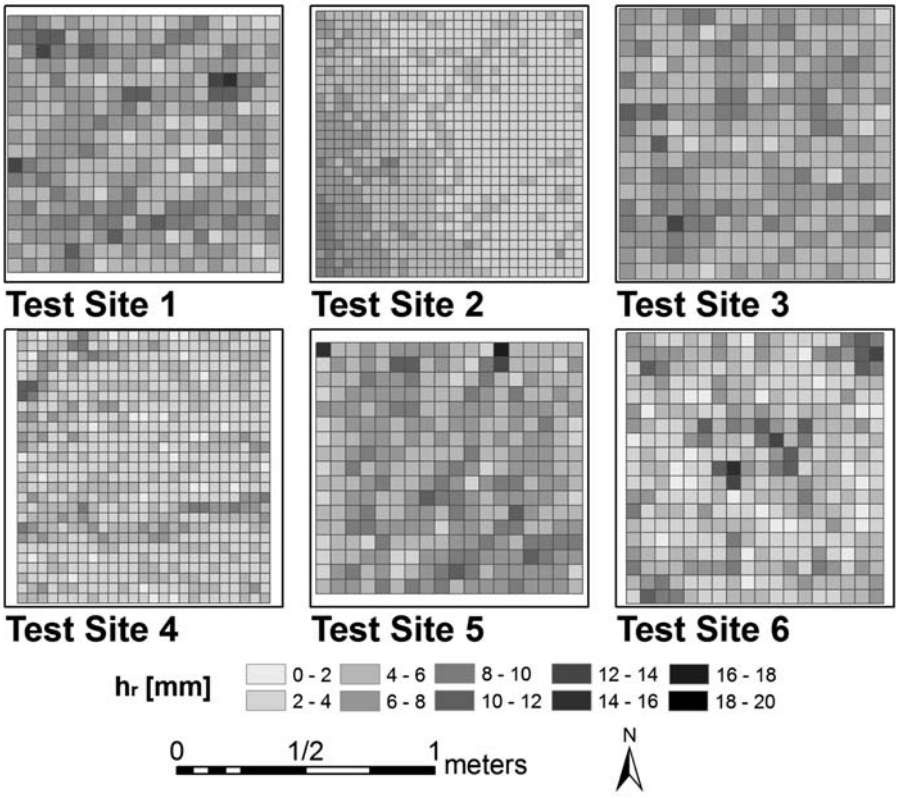

Fig. 5. Grid of data set "5scans" for all six test sites of study site Gumpe (h_r = effective roughness height). Grid cell size varies due to changes in the largest clast size.

Table 1. Median of roughness height (h_r) for all data sets lscan_a, lscan_b, etc.) at study site Gumpe, STD = standard deviation.

dataset	median of h_r [mm]					
	Test Site 1	Test Site 2	Test Site 3	Test Site 4	Test Site 5	Test Site 6
1Scan_a	7.6	2.7	8.1	5.3	8.0	5.6
1Scan_b	7.5	3.1	8.0	5.4	8.2	5.7
1Scan_c	7.2	3.1	7.9	5.6	7.8	5.5
1Scan_d	7.5	2.9	8.0	5.3	7.9	5.7
1Scan_e	7.1	2.7	8.0	5.0	7.9	5.6
2Scans_a	8.4	3.0	8.0	5.6	8.1	6.2
2Scans_b	7.7	3.4	8.3	5.5	8.3	5.9
3Scans	8.3	4.2	8.0	5.6	8.2	6.1
4Scans	8.1	3.3	7.9	5.7	8.2	6.1
5Scans	8.2	4.0	8.0	5.7	8.3	6.2
STD	0.5	0.5	0.1	0.2	0.2	0.3

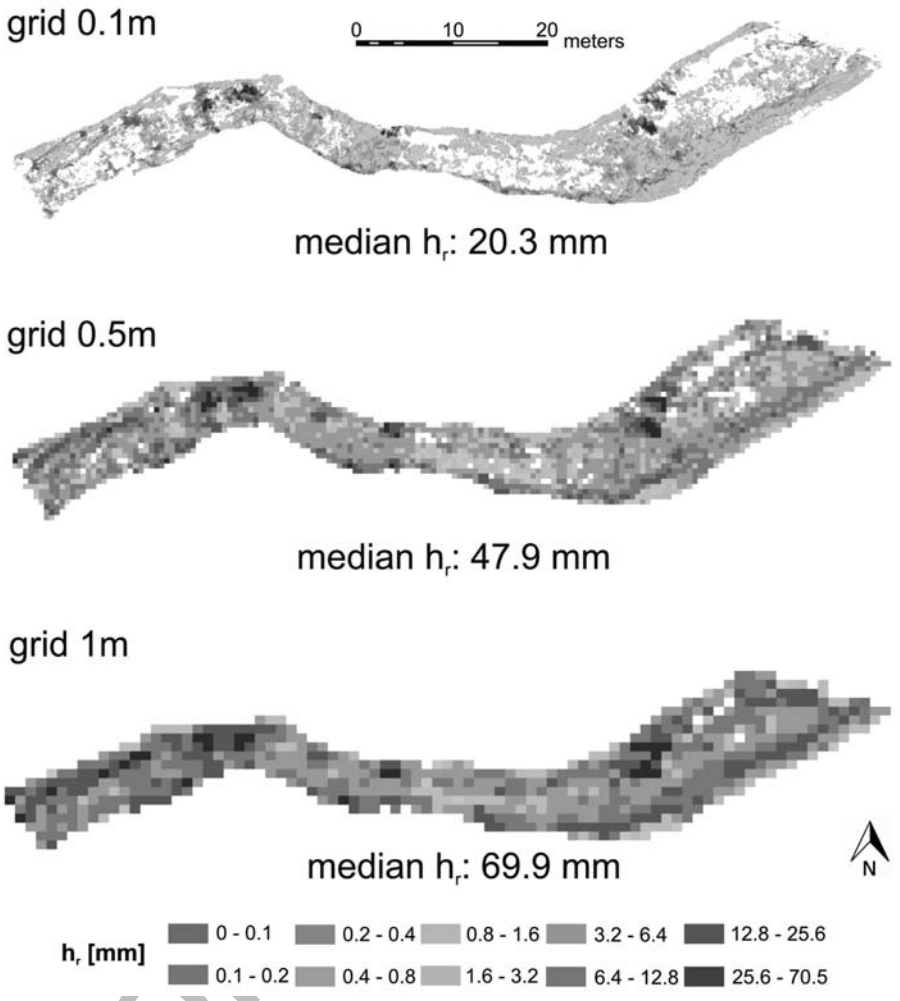

Fig. 6. Grids for the three data sets with different cell sizes from study site Sieben Sprünge (h_r = effective roughness height)

were within the range accuracy of the scanner. This result suggests that despite particle shading, the number of scans used to calculate surface roughness is relatively unimportant.

Study site Sieben Sprünge was chosen to analyse the influence of the grid cell size on the calculation of surface roughness heigth. The river obstructed the laser reducing data coverage at this site. Obstructed areas were acounted for in post-processing by increasing the grid cell size thus increasing the probability of at least two points lying within each individual grid cell. This however, leads to roughness calculation errors as h_r values systematically increase with increased grid cell size (Fig. 6). For small grid cell sizes, the range in elevations contained within a single cell may not accurately reflect the true roughness length at the test site. As a result h_r values systematically decrease with a reduction in grid cell size. The median values of h_r for all three data sets show sub-

Table 2. Characteristic data of the linear regression of study site Gumpe (m = regression coefficient, r = correlation coefficient).

data set	Test Site 1		Test Site 2		Test Site 3		Test Site 4		Test Site 5		Test Site 6	
	m	r	m	r	m	r	m	r	m	r	m	r
1Scan_a	1.34	0.982	2.59	0.996	1.49	0.961	1.02	0.977	1.72	0.985	1.37	0.992
1Scan_b	1.26	0.982	1.61	0.984	1.43	0.968	1.20	0.993	1.35	0.991	1.35	0.993
1Scan_c	1.19	0.959	1.57	0.967	1.42	0.995	1.47	0.988	1.82	0.982	1.36	0.997
1Scan_d	1.46	0.974	2.23	0.990	1.64	0.994	1.38	0.986	1.48	0.994	1.50	0.991
1Scan_e	1.41	0.992	2.99	0.994	1.34	0.972	0.97	0.969	1.41	0.998	1.44	0.997
2Scans_a	1.5	0.988	1.71	0.961	1.58	0.991	1.20	0.974	1.86	0.987	1.42	0.994
2Scans_b	1.55	0.98	1.76	0.990	1.47	0.983	1.23	0.991	1.41	0.996	1.39	0.996
3Scans	1.56	0.975	1.21	0.977	1.35	0.990	1.15	0.984	1.65	0.996	1.38	0.997
4Scans	1.45	0.956	1.85	0.986	1.67	0.994	1.10	0.964	1.78	0.997	1.39	0.997
5Scans	1.52	0.976	1.50	0.980	1.65	0.992	1.30	0.981	1.56	0.996	1.40	0.996

stantial differences (Fig. 6). The h_r value for the 0.1 m cell size is 20.3 mm, the value for the 0.5 m cell size is 47.9 mm and for the largest cell size of 1 m the h_r value is 69.9 mm. It is clear that there are significant differences between the roughness values for all data sets indicating that roughness calculation is highly dependent on grid cell size.

4.3 *Comparison between TLS-derived data and the particle sampling method*

A linear regression function was used to compare c-axis percent classes and $2h_r$ values for the TLS-derived data and the collected particle samples. The results from study site Gumpe are listed in Table 2. For all data sets, the correlation is very good (e.g., $r = 0.991$), indicating a strong linear relationship between the c-axis and $2h_r$ classes. This is confirmed by a very high significance of the regression model ($p = 0.0001$). For Test Sites 5 and 6 the c-axis is represented very well by the laser scanning data.

Significant differences in h_r values can be identified by comparing the data sets from each test site. The slope of the regression function (regression coefficient m) and the coefficient of determination (R^2) were used to compare the c-axis of sampled particles and scanner-derived $2h_r$ data. The high value of R^2 shows that the linear relationship between $2h_r$ and the c-axis is very strong. Furthermore, the slope of the regression shows that there is no 1:1 relationship between both variables. For this reason, it can be said that TLS-data is more appropriate for representing surface roughness. For all test sites (excluding site 2), sufficient results were found for the data sets containing only one scan suggesting that the determination of the surface roughness is possible using only one scan.

At study site Sieben Sprünge both variables (c-axis and $2h_r$) were compared for each data set. With increasing cell size the measured values of the c-axis are better predicted by the regression function (Fig. 7). The R^2 value increases from 96 % (cell size 0.1 m) to 99.27 % (cell size 1 m) and the slope of the regression function decreases. For all three cell sizes the linear relationship between c-axis and $2h_r$ is strong ($p = 0.0001$). However, the slope of the regression function is much less than one (m = 0.15–0.35) suggesting that there is no 1:1 relationship between c-axis and $2h_r$.

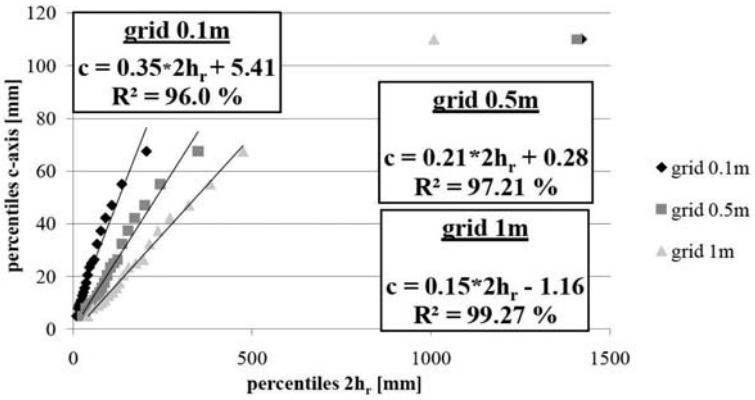

Fig. 7. Comparison between TLS-derived data (x-axis) and the particle c-axis values (y-axis) for study site Sieben Sprünge (Outliers are not taken into account for the regression function).

5 *Discussion*

For the grain size distribution at study site Gumpe, channel bed roughness quantification by TLS is not dependent on the number of scans made. This conclusion is drawn from the minimal deviations in h_r values calculated for the ten data sets from each test site (Table 1). In all cases, good correlation was found between TLS data and sediment samples deviation. However, measured and calculated data were found to diverge for small and large values (Fig. 8). The reason for this is that exceptionally small and large particles are not measured while using conventional sampling methods (WOLMAN 1954, BUNTE & ABT 2001). The laser scanner does not have this problem as it records all particles from a given surface.

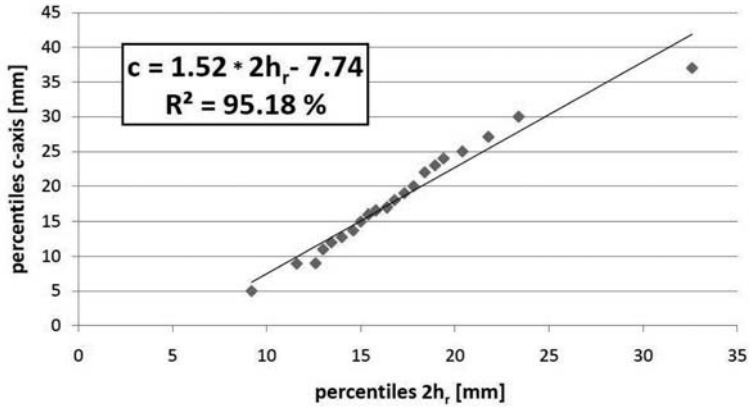

Fig. 8. Comparison between TLS-derived data (x-axis) and the particle c-axis values (y-axis) for test site 1 (data set "5scans") of study site Gumpe.

The deviations between the h_r values of the different data sets may arise for a variety of reasons. Various systematic errors can occur while scanning. One of these errors is caused by the positional inaccuracy of the laser scanner. According to Optech (2012) the positional inaccuracy increases 8 mm per 100 m. Other systematic errors may occur in post-processing during the merging process (Fig. 3). Pesci et al. (2011) suggest another source of error arises from the similarity between user-selected point spacing and the beam diameter (ca. 12 mm) because the resolution of a scan must always lie between these two values. Small differences between the data sets can also be caused by the different scanning positions. From certain (azimuthal) directions particles are visible which cannot be seen from other positions due to particle shading. In addition, the angle of incidence will also alter the extent of burial or imbrication seen by the scanner.

The influence of the grid cell size on roughness calculation was assessed at study site Sieben Sprünge. The smaller the chosen grid edge length is, the smaller the area covered by a single grid cell. With increasing cell size the number of points within a cell rises. For this reason, the difference in height between those points is larger than the difference for smaller grid cell sizes. In this situation, the calculated roughness values are also higher. With increasing cell size the R^2 value for the linear regression also increases. This suggests a dependency on grid cell size. The grid cell size in turn depends on the grain size distribution in the scan area. Thus, grid cell size selection must be optimized for grain size distribution. The slope of the regression is significantly below one for all data sets. That is because the larger particles located on this study site were not measured by particle sampling. In addition, a poorly chosen cell size may account for this error made during sampling (Wolman 1954, Bunte & Abt 2001).

6 *Conclusions*

In this study we investigated whether the application of TLS is suitable for the determination of channel bed roughness in an alpine river bed. This study specifically examined how different parameters (number of scans, grid cell size) influence this method of roughness calculation.

Unlike methods based on particle sampling, TLS-derived data allow the calculation of surface roughness for an entire area and not just for individual segments. Using traditional approaches, roughness is determined via characteristic grain size (e.g., D_{84}). The c-axis is considered as one of the dominant contributors to the actual roughness height (Nikora et al. 1998). For this reason methods based on the grain size produce unrealistic results. In addition, particles in the channel bed are often covered by other particles or buried in finer sediments. This results in a systematic error if the particles are removed by hand during sampling. Terrestrial laser scanners detect the actual heights of the channel bed and consider the orientation of particles.

An important consideration when using TLS is the number of scans needed to prevent shadowing effects. Our results show there are no significant differences in average roughness values generated from data sets containing one, or up to five individual scans. Additionally, the comparison of the TLS data with sediment samples shows that there is only little discrepancy between the different data sets within a single test site. For this reason, one recorded scan is sufficient to determine bed roughness.

The results of study site Sieben Sprünge show a connection between calculated grain roughness and grid cell size. The roughness values increase with cell size. This leads to large deviations

from the sampled c-axis values. In addition, the coefficient of determination found by regression analysis on $2h_r$ and c-axis data increases with cell size. Thus, we conclude that the determination of bed surface roughness is highly dependent on the grid cell size.

This study has enhanced our understanding of the methods for roughness determination via terrestrial laser scanning. Roughness determination via TLS data does not depend significantly on the number of scans. In contrast, the calculation of surface roughness depends heavily on the grid cell size chosen during post processing.

Acknowledgements

This study was supported by the German Research Foundation (DFG-project "Effects of extreme events on the function of sediment stores and sediment sources, on sediment mobility and transport in an Alpine river system", grant to Karl-Heinz Schmidt, SCHM 472/15-1). Alexander Bryk was supported by the internship program IAESTE of the German Academic Exchange Service (DAAD) (Ref. Code: DE-12-1191-A-1). We thank our two anonymous reviewers for their constructive comments.

References

Aberle, J. & Smart, G. M. (2003): The influence of roughness structure on flow resistance on steep slopes. – J. Hydraul. Res. **41** (3): 259–269, doi: 10.1080/00221680309499971.

Bathurst, J. C. (1985): Flow resistance estimation in mountain rivers. – J. Hydraul. Engin. **111** (4): 625–643, doi: 10.1061/(ASCE)0733-9429(1985)111:4(625).

Bimbŏse, M., Nicolay, A., Bryk, A. Schmidt, K.-H. & Morche, D. (2011) Investigations on intra- and inter-annual coarse sediment dynamics in a high-mountain river. – Z. Geomorph. N.F. Suppl. **55** (2): 67–80, doi: 10.1127/0372-8854/2011/0055S2-0046.

Boyer, M. C. (1954): Estimating the Manning coefficient from an average bed roughness in open channels. – Transact. Amer. Geophys. Union **35** (6): 957–961.

Buckley, S. J., Schwarz, E., Terlaky, V., Howell, J. A. & Arnott, R. W. C. (2009): Terrestrial Laser Scanning combined with Photogrammetry for Digital outcrop modelling. – In: Bretar, F., Pierrot-Deseilligny, M. & Vosselmann, G. (eds.) (2009): Laser scanning 2009, ISPRS **38** (3/W8): 75–80.

Bunte, K. &. Abt, S. R. (2001): Sampling Surface and Subsurface Particle-Size Distributions in Wadable Gravel- and Cobble-Bed Streams for Analyses in Sediment Transport, Hydraulics, and Streambed Monitoring. – Gen. Tech. Rep. RMRS-GTR-74: 428 pp., U.S. Dep. Agricult., For. Serv., Rocky Mountain Res. Stat., Fort Collins.

Comiti, F., Cadol, D. & Wohl, E. E. (2009): Flow regimes, bed morphology, and flow resistance in self-formed step-pool channels. – Wat. Resour. Res. **45:** W04424, doi: 10.1029/2008WR007259.

Conforti, D., Deline, P., Mortara, G. & Tamburini, A. (2005): Terrestrial Scanning Lidar Technology applied to study the evolution of the ice-contact Miage Lake (Mont Blanc, Italy). 9th Alpine Glaciological Meeting, 24th and 25th February, Milan.

Eitelmann, A. & Morche, D. (2011): Untersuchungen zu Totholzablagerungen und deren Einfluss auf die Gerinnemorphologie in einem Hochgebirgsbach. – Hallesches Jahrb. Geowiss. **32/33:** 83–96.

Furbish, D. J. (1987): Conditions for geometric similarity of coarse stream-bed roughness. – Math. Geol. **19** (4): 291–307, doi: 10.1007/BF00897840.

Götz, J. & Schrott, L. (eds.) (2010): Das Reintal – Geomorphologischer Lehrpfad am Fuße der Zugspitze. – Pfeil, München.

Gomez, B. (1993): Roughness of Stable, Armored Gravel Beds. – Wat. Resour. Res. **29** (11): 3631–3642, doi: 10.1029/93WR01490, 1993.

Heckmann, T., Haas, F., Wichmann, V. & Morche, D. (2008): Sediment budget and morphodynamics of an alpine talus cone on different timescales. – Z. Geomorph. N.F. Suppl. **52** (1): 103–121, doi: 10.1127/0372-8854/2008/0052S1-0103.

Heckmann, T., Bimböse, M., Krautblatter, M., Haas, F., Becht, M. & Morche, D. (2012): From geotechnical analysis to quantification and modeling using LiDAR data: A study on rockfall in the Reintal catchment, Bavarian Alps, Germany. – Earth Surf. Proc. Landf. **37** (1): 119–133, doi: 10.1002/esp.2250.

Heritage, G. L. & Milan, D. J. (2009): Terrestrial Laser Scanning of grain roughness in a gravel-bed river. – Geomorphology **113** (1–2): 4–11, doi: 10.1016/j.geomorph.2009.03.021.

Heritage, G. & Hetherington, D. (2005): The use of high-resolution field laser scanning for mapping surface topography in fluvial systems. – IAHS Publ. **291:** 269–271.

Heritage, G. L. & Hetherington, D. (2007): Towards a protocol for laser scanning in fluvial geomorphology. – Earth Surf. Proc. Landf. **32** (1): 66–74, doi: 10.1002/esp.1375.

Hey, R. D. (1979): Flow resistance in gravel-bed rivers. – J. Hydraul. Div. ASCE **105** (4): 365–379.

Hodge, R., Brasington, J. & Richards, K. S. (2009): In situ characterization of grain-scale fluvial morphology using terrestrial laser scanning. – Earth Surf. Proc. Landf. **34** (7): 954–968, doi: 10.1002/esp.1780.

Krautblatter, M., Moser, M., Schrott, L., Wolf, J. & Morche, D. (2012): Significance of rockfall magnitude and carbonate dissolution for rock slope erosion and geomorphic work on Alpine limestone cliffs (Reintal, German Alps). – Geomorphology **167–168:** 21–34, doi: 10.1016/j.geomorph.2012.04.007.

Lee, A. J. & Ferguson, R. I. (2002): Velocity and flow resistance in step-pool streams. – Geomorphology **46** (1–2): 59–71, doi: 10.1016/S0169-555X(02)00054-5.

Mazzarini, F., Favalli, M., Isola, I., Neri, M. & Pareschi, M. T. (2008): Surface roughness of pyroclastic deposits at Mt Etna by 3 d laser scanning. – Ann. Geophys. **51** (5/6): 813–822, doi: 10.4401/ag-4461.

Milan, D. J., Heritage, G. L. & Hetherington, D. (2007): Application of a 3 D laser scanner in the assessment of erosion and deposition volumes and channel change in a proglacial river. – Earth Surf. Proc. Landf. **32** (11): 1657–1674, doi: 10.1002/esp.1592.

Montgomery, D. R. & Buffington, J. M. (1997): Channel-reach morphology in mountain drainage basins. – Geol. Soc. Amer. Bull. **109** (5): 596–611, doi: 10.1130/0016-7606(1997)109<0596:CRMIMD>2.3.CO,2.

Morche, D., Katterfeld, C., Fuchs, S. & Schmidt, K.-H. (2006): The life-span of a small high mountain lake, the Vordere Blaue Gumpe in Upper Bavaria, Germany. – IAHS Publ. **306:** 72–81, IAHS Press, Wallingford.

Morche, D. & Schmidt, K.-H. (2005): Particle size and particle shape analyses of unconsolidated material from sediment sources and sinks in a small Alpine catchment (Reintal, Bavarian Alps, Germany). – Z. Geomorph. N.F. Suppl. **138:** 67–80.

Morche, D. & Schmidt, K.-H. (2012): Sediment transport in an alpine river before and after a dambreak flood event. – Earth Surf. Proc. and Landf. **37** (3): 347–353, doi: 10.1002/esp.2263.

Morche, D., Schmidt, K.-H, Heckmann, T. & Haas, F. (2007): Hydrology and geomorphic effects of a high-magnitude flood in an Alpine river. – Geograf. Ann. **89** A (1): 5–19, doi: 10.1111/j.1468-0459.2007.00304.x.

Morche, D., Witzsche, M. & Schmidt, K.-H. (2008): Hydrogeomorphological characteristics and fluvial sediment transport of a high mountain river (Reintal Valley, Bavarian Alps, Germany). – Z. Geomorph. N.F. Suppl. **52** (1): 51–77, doi: 10.1127/0372-8854/2008/0052S1-0051.

Nikora, V. I., Goring, D. G. & Biggs, B. J. F. (1998): On gravel-bed roughness characterization. – Wat. Resour. Res. **34** (3): 517–527, doi: 10.1029/97WR02886, 1998.

Nikuradse, J. (1933): Strömungsgesetze in rauhen Röhren. – VDI-Forschungsheft 361, Beilage zu Forschung auf dem Gebiet des Ingenieurwesens, Ausgabe B, **4:** 24 pp.

Optech Inc. (2012): http://www.optech.ca/i3dtechoverview-ilris.htm.12-01-19.

Pesci, A., Loddo, F. & Conforti, D. (2007): The first terrestrial laser scanner application over Vesuvius: High resolution model of a volcano crater. – Int. J. Rem. Sens. **28:** 203–219, doi: 10.1080/01431160500534473.

Pesci, A., Teza, G. & Bonali, E. (2011): Terrestrial laser scanner resolution: numerical simulations and experiments on spatial sampling optimization. – Rem. Sens. **3:** 167–184, doi: 10.3390/rs3010167.

Pignatelli, C., Piscitelli, A., Damato, B. & Mastronuzzi, G. (2010): Estimation of the value of Manning's coefficient using Terrestrial Laser Scanner techniques for the assessment of flooding by extreme waves. – Z. Geomorph. N.F. Suppl. **54** (3): 317–336, doi: 10.1127/0372-8854/2010/0054S3-0030.

Rabatel, A., Deline, P., Jaillet, S. & Ravanel, L. (2008): Rock falls in high-alpine rock walls quantified by terrestrial lidar measurements: A case study in the Mont Blanc area. – Geophys. Res. Lett. **35:** L10502, doi: 10.1029/2008GL033424, 2008.

Reid, D. E. & Hickin, E. J. (2008): Flow resistance in steep mountain streams. – Earth Surf. Proc. Landf. **33** (14): 2211–2240, doi: 10.1002/esp-1682.

Robert, A. (2011): Flow resistance in alluvial channels. – Progr. Phys. Geogr. **35** (6): 765–781, doi: 10.1177/0309133311414604.

Sass, O., Krautblatter, M. & Morche, D. (2007): Rapid lake infill following major rockfall bergsturz events revealed by ground-penetrating radar GPR measurements Reintal German Alps. – The Holocene **17** (7): 965–976, doi: 10.1177/0959683607082412.

Schmidt, K.-H. & Morche, D. (2006): Sediment output and effective discharge in two small high mountain catchments in the Bavarian Alps, Germany. – Geomorphology **80:** 131–145, doi: 10.1016/j.geomorph.2005.09.013.

Schrott, L., Götz, J., Geilhausen, M. & Morche, D. (2006): Spatial and temporal variability of sediment transfer and storage in an Alpine basin (Bavarian Alps, Germany). – Geographica Helvetica **61** (3): 191–200.

Smart, G. M., Aberle, J., Duncan, M. & Walsh, J. (2004): Measurement and analysis of alluvial bed roughness. – J. Hydraul. Res. **42** (3): 227–237, doi: 10.1080/00221686.2004.9728388.

van Rijn, L. C. (1984): Sediment transport, Part III: Bed forms and alluvial roughness. – J. Hydraul. Eng. **110** (12): 1733–1754, doi: 10.1061/(ASCE)0733-9429(1984)110:12(1733).

Wolman, M. G. (1954): A method of sampling coarse river-bed material. – Transact. Amer. Geophys. Union **35** (6): 951–956.